

EXPERIMENTAL PROGRESS: CURRENT FILAMENTATION INSTABILITY STUDY *

Brian Allen[#], Patric Muggli, University of Southern California, Los Angeles CA 90089, USA
 Joana Martins, Luís O. Silva, GoLP/Instituto de Plasmas e Fusão Nuclear – Laboratório Associado,
 Instituto Superior Técnico, Lisboa 1049-001, Portugal
 Vitaly Yakimenko, Mikhail Fedurin, Karl Kusche, Marcus Babzien, Brookhaven National
 Laboratory, Upton NY 11973, USA
 Chengkun Huang, Los Alamos National Laboratory, Los Alamos NM 87545, USA
 Warren Mori, University of California at Los Angeles Los Angeles, CA 90095, USA

Abstract

Current Filamentation Instability, CFI, is of central importance for the propagation of relativistic electron beams in plasmas. CFI has potential relevance to astrophysics, magnetic field and radiation generation in the afterglow of gamma ray bursts, and inertial confinement fusion, energy transport in the fast-igniter concept. An experimental study of this instability is underway at the Brookhaven National Laboratory – Accelerator Test Facility. We use the particle-in-cell code QuickPIC to study phenomena observed in the experiment. These include merging of filaments and the dependence of the growth rate of the instability on plasma density and beam emittance.

INTRODUCTION

Current Filamentation Instability, CFI, is a basic beam-plasma instability that has a purely imaginary frequency and is purely transverse electromagnetic. It occurs due to non-uniformities in the transverse beam and plasma profiles, which lead to unequal opposite beam current and plasma return current and to the generation or enhancement of transverse magnetic fields. The resulting $\mathbf{v} \times \mathbf{B}$ force (\mathbf{v} - velocity of the beam or plasma return current and \mathbf{B} - magnetic field) amplifies the non-uniformity of the current and drives the instability. As a result the beam breaks up into filaments with size and spacing on the order of the cold plasma collisionless skin depth, c/ω_{pe} (c – speed of light in vacuum and ω_{pe} – the angular plasma electron frequency).

The phenomena responsible for Gamma Ray Bursts (GRB's) and their associated afterglow are largely unknown. One proposed theory for the afterglow is the Fireball theory [1]. In this theory, as matter (consisting of electrons, positrons and ions) is ejected from the GRB, relativistic collisionless shocks occur between this matter resulting in the generation of large magnetic fields and radiation. The generation of magnetic fields and radiation could possibly be explained through the occurrence of the CFI.

In the Inertial Confinement Fusion, ICF, concept the compression and ignition of a deuterium and tritium fuel pellet is accomplished in a single process. The ability to separate ICF into two processes could reduce the strict

requirements for the pellet fabrication tolerances and pellet illumination symmetry requirements. The Fast-Igniter ICF [2, 3] concept uses a guiding metal cone manufactured into the fuel pellet. When compression of the fuel pellet reaches the critical density a short high intensity laser pulse is focused into the cone. A beam of hot electrons is generated near the critical surface and the hot electrons then propagate to the core where they ignite the fusion process. The presence of CFI for this beam of hot electrons could affect the transport and energy deposition location.

The regime where CFI can occur is determined by two parameters, (1) the transverse beam size (σ_r) relative to the plasma skin depth and (2) the Lorentz factor, γ_0 , of the beam. For the case where the transverse beam size is smaller than the plasma skin depth ($\sigma_r < c/\omega_{pe}$) the plasma return current flows outside the beam, this is a regime particularly favorable for Plasma WakeField Accelerators (PWFA) and CFI does not occur. When the transverse beam size is larger than the plasma skin depth ($\sigma_r > c/\omega_{pe}$) the return current passes through the beam, creating a situation where CFI can occur. In general, the beam is subject to instabilities with a wavenumber, \mathbf{k} , at an arbitrary angle with respect to the beam propagation velocity, \mathbf{v}_b . Linear analysis [4] reveals that for low γ_0 beams, the dominant instability is a two stream electrostatic instability with $\mathbf{k} \parallel \mathbf{v}_b$. For relativistic beams, $\gamma_0 \gg 1$, the dominant instability is the CFI. Simulations reveal that for the finite transverse beam size case (Reference 4 is for the case of an infinite transverse beam size) CFI dominates and the filament size and spacing are on the order of the plasma skin depth. The growth rate of the instability [5] is: $\Gamma = v_b/c(n_b/n_e\gamma_0)^{1/2}\omega_{pe} \sim n_b^{1/2}$ and is seen to be dependent on the beam density, n_b , and independent of the plasma density, n_e (as long as $\sigma_r > c/\omega_{pe}$).

EXPERIMENT

An experiment is underway at the Brookhaven National Laboratory – Accelerator Test Facility, BNL-ATF. The ATF was chosen for its ability to create a regime favorable to CFI ($\sigma_r > c/\omega_{pe}$ and $\gamma_0 \gg 1$) with its 60 MeV electron beam and also allow for the study of the instability as a function of beam density (Q – beam charge) and plasma density, n_e . Parameters for the ATF

*Work supported by NSF grant 0903822

[#]brianall@usc.edu

over-compressed e^- beam are outlined in references [6, 7]. The plasma at the ATF is produced in a capillary discharge with diameter of 0.8mm, length 2cm and densities in the range of $10^{15} < n_e < 10^{18} \text{ cm}^{-3}$. An imaging system was designed [8] and implemented to image the transverse beam profile at the capillary/plasma exit with a resolution of 1.9 μm RMS.

For CFI, the number and size of filaments scale with the plasma density and hence plasma skin depth, $c/\omega_p \sim n_e^{-1/2}$. In the analysis of experimental data we observed that as the plasma density increases (c/ω_p decreases) we transition from single filaments for $1.1 < \sigma_y/(c/\omega_p) < 2.2$ to multiple (one to five) filaments for $2.2 < \sigma_y/(c/\omega_p) < 4.5$, all filaments on average scaled with the plasma skin depth. As the plasma density increases beyond $\sigma_y/(c/\omega_p) > 4.5$ only one and two filaments are observed and do not scale with the plasma skin depth. From theory, for the case of infinite transverse size, we would expect a continued increase in the number of filaments while maintaining the scaling relationship. This deviation could be due to merging of the filaments as is seen in simulations [9]. We will look at the evolution of the instability and explore its dependence on plasma density and beam emittance.

SIMULATION SETUP

Simulations were performed with particle-in-cell (PIC) code QuickPIC [10] for the BNL-ATF over-compressed e^- beam parameters with a uniform plasma density. Simulation parameters are shown in Table 1 and were chosen to compliment prior experimental studies [11]. The experimental program introduced two changes to the original simulation parameters. The first change is from a symmetric beam ($\sigma_{x,y}=100 \mu\text{m}$) to an asymmetric beam ($\sigma_x=100\mu\text{m}$ and $\sigma_y=62.5 \mu\text{m}$). This was chosen to maintain the same transverse size ratio as in the experiment. To maintain the same beam density as in prior simulations, due to the reduced beam size in the y-dimension, the charge in the beam was reduced (from $Q=200\text{pC}$ to $Q=125\text{pC}$). The second change was an increase in the normalized emittance of the beam due to the introduction of a pellicle along the beam line (which increases the emittance from $\epsilon_{N,x,y}=1\text{--}2\text{mm-mrad}$ to $\epsilon_{N,x,y}=4\text{--}8\text{mm-mrad}$.)

Table 1: Simulation Parameters

Parameter	Value
σ_x –RMS Transverse Size (μm)	100
σ_y –RMS Transverse Size (μm)	62.5
σ_z –RMS Bunch Length (μm)	30
$\epsilon_{N,x,y}$ - Normalized Emittance (mm-mrad)	4 to 8
γ_0 – Lorentz Factor	117
Q – Bunch Charge (pC)	100 to 200

Simulation Box – Dimensions (μm)	1,100x1,100x160
Simulation Box – Cells (number)	512x512x128

SIMULATION RESULTS

We will first look at the evolution of the beam at three propagation lengths for two plasma densities (all beam parameters are constant: $Q=125\text{pC}$ and $\epsilon_{N,x,y}=4\text{mm-mrad}$). The beam density evolution is shown in Figure 1 and we see the number of filaments depends on the plasma density. By 3.5cm of plasma merging of filaments is observed for both plasma densities. Prior to merging the filaments are of size c/ω_p , but after merging the resulting filaments become larger than c/ω_p .

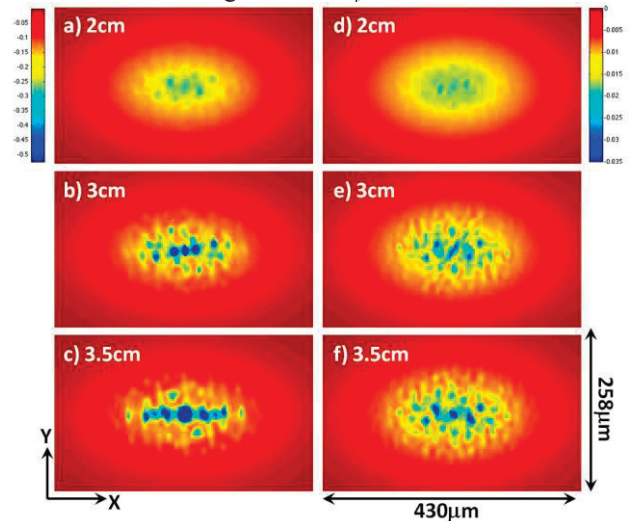


Figure 1: Evolution of the instability: images of the transverse beam density for $Q=125\text{pC}$ and $\epsilon_{N,x,y}=4 \text{ mm-mrad}$. $n_e=5.0 \times 10^{17} \text{ cm}^{-3}$ for a) through c) and $1.0 \times 10^{18} \text{ cm}^{-3}$ for d) through f).

Previously we showed [11] that for a constant plasma density the growth rate increased with the beam density (simulations were for a transversely symmetric beam, but are consistent for the asymmetric beam). The magnetic energy for three different plasma densities and constant beam parameters ($Q=125\text{pC}$ and $\epsilon_{N,x,y}=4 \text{ mm-mrad}$) is shown in Figure 2. The growth rate, Γ , (the slope of the linear portion of the exponential fit to the logarithmic magnetic energy) for the three plasma densities indicates that the growth rate increases with plasma density. The growth length, c/Γ , increases from 4.2mm for $n_e=5.0 \times 10^{17} \text{ cm}^{-3}$ to 4.9mm for $n_e=1.0 \times 10^{18} \text{ cm}^{-3}$. Figure 2 also shows that saturation occurs quicker (over shorter distance) at higher plasma densities. While not a large effect it does show that plasma density plays a role in the growth of the instability.

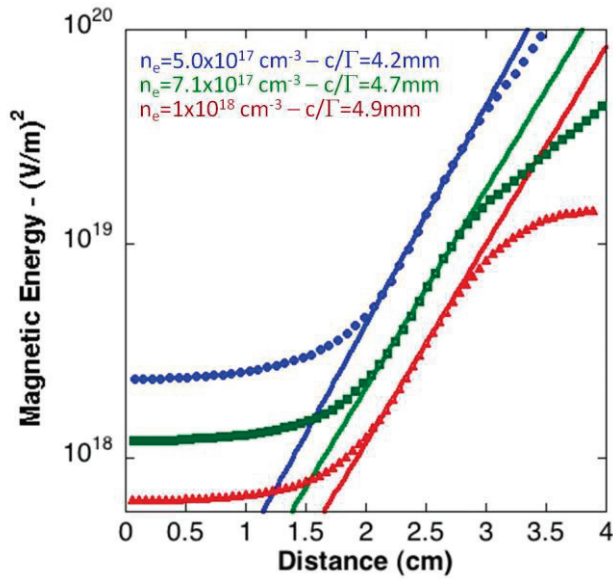


Figure 2: Effect of plasma density on growth in magnetic energy for $Q=125\text{pC}$ and $\epsilon_{N_{x,y}}=4\text{mm-mrad}$. Plasma density, n_e , blue: $5.0 \times 10^{17} \text{cm}^{-3}$, green: $7.1 \times 10^{17} \text{cm}^{-3}$ and red: $1.0 \times 10^{18} \text{cm}^{-3}$.

Emittance of the beam competes with the instability and if high enough can suppress it [9]. The incoming beam emittance increased by up to a factor of 8x from the initial beamline configuration. Simulations show a significant increase in the growth length from 4.7mm for $\epsilon_{N_{x,y}}=4\text{mm-mrad}$ to 8.4mm for $\epsilon_{N_{x,y}}=8\text{mm-mrad}$. Figure 3 shows the transverse evolution of the beam density for the $\epsilon_{N_{x,y}}=8\text{mm-mrad}$ case. Comparing Fig. 3 to Fig. 1 a) to c) we see the instability is suppressed due to the increased emittance and this could limit the experiment.

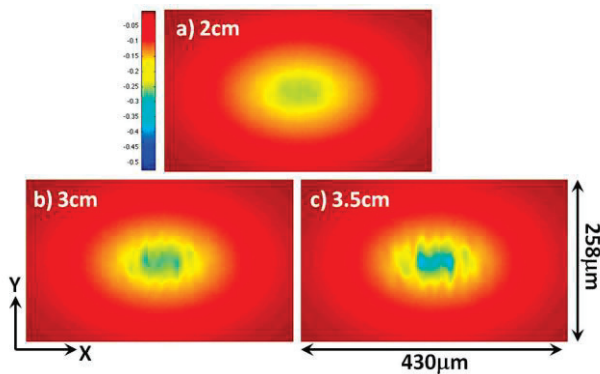


Figure 3: Transverse evolution of beam density ($n_e=7.1 \times 10^{17} \text{cm}^{-3}$, $Q=125\text{pC}$ and $\epsilon_{N_{x,y}}=8\text{mm-mrad}$) showing suppression of CFI.

Table 2: Growth length, c/Γ , estimated from simulations

Emittance (mm-mrad)	Plasma Density (cm^{-3})		
	5.0×10^{17}	7.1×10^{17}	1.0×10^{18}
4	4.2	4.7	4.9
8	8.4		
Theoretical	3.5mm	3.5mm	3.5mm

CONCLUSION

In summary, we have looked at the growth length of the instability as a function of plasma density and emittance. Table 2 summarizes the results and compares them to the theoretical growth length. We observe merging of the filaments leading to a reduction in number and not scaling with the skin depth. There is a dependence of the growth rate on plasma density, which is not predicted in theory and Γ increases with increased plasma density. Finally, we see that the increase in emittance in the experiment slows the growth of the instability, as is expected and could be a limiting factor in the experiment.

ACKNOWLEDGEMENTS

This work was supported by NSF grant 0903822 and DoE grant DEFG03-92ER40745. Simulations were conducted on HPCC at the University of Southern California and on NERSC. The authors would also like to thank the UCLA/IST collaboration team for access to QuickPIC and their support.

REFERENCES

- [1] C. Deutsch et al., *Transp. Thry and Stat. Phys.*, Volume 34, Issue 3 - 5, 353 (2005)
- [2] G. Cavallo and M.J. Rees, *Royal Astro. Society, Mnthly Ntes*, 183, 359 (1978).
- [3] Y. Sentoku et al., *Phys. Rev. Lett.* 90, 155001 (2003)
- [4] A. Bret et al., *The Astro. Jrnl*, Volume 699, Number 2, (2009)
- [5] A. Bret et al., *Phys. Rev. Lett.* 94, 115002 (2005)
- [6] W.D. Kimura et. al, *AIP Conf. Prcds.* Volume 877, 534 (2006)
- [7] B. Allen et al., *AIP Conf. Prcds.* Volume 1299 (2010)
- [8] B. Allen et. al., *PAC Conf. Prcds.* Pg. 1719-1720 (2011).
- [9] J. J. Su et. al. *IEEE Trans. on Plasma Science* 15, 2 (1987).
- [10] C. Huang et. al. *Jrnl. of Comp. Phys.*, Volume 217, Issue 2 (2006).
- [11] B. Allen et. al. *PAC Conf. Prcds.* (2008).